SCIENCE CHINA
Technological Sciences

Special Topic: Network and Control Engineering
•Article•

November 2023 Vol.66 No.11: 3139–3152
https://doi.org/10.1007/s11431-023-2441-5

Energy flow accounts for the adaptive property of functional synapses

WU FuQiang[1,2], GUO YiTong[3] & MA Jun[1,3,4*]

[1] *Department of Physics, Lanzhou University of Technology, Lanzhou 730050, China;*
[2] *School of Mathematics and Statistics, Ningxia University, Yinchuan 750021, China;*
[3] *College of Electrical and Information Engineering, Lanzhou University of Technology, Lanzhou 730050, China;*
[4] *School of Science, Chongqing University of Posts and Telecommunications, Chongqing 400065, China*

Received April 6, 2023; accepted May 31, 2023; published online October 17, 2023

In the presence of external stimuli and electromagnetic radiation (EMR), biological neurons can exhibit different firing patterns and switch to appropriate firing modes because of intrinsic self-adaption. Coupling to memristive synapses can discern the EMR effect, and memristive synapses connecting to neurons can be effectively regulated by external physical fields. From a dynamical viewpoint, the appropriate setting for memristive synapse intensity can trigger changes in neural activities; however, the biophysical mechanism of adaptive regulation in the memristive biophysical neuron has not been clarified. Herein, a memristor is used to control a simple neural circuit by generating a memristive current, and an equivalent memristive neuron model is obtained. A single firing mode can be stabilized in the absence of EMR, while multiple firing modes occur in the neuron under EMR. The gain of the memristive synaptic current is dependent on the energy flow, and the shunted energy flow in the memristive channel can control the energy ratio between the electric field and magnetic field. The growth and enhancement of the memristive synapse depend on the energy flow across the memristive channel. The memristive synapse is enhanced when its field energy is below the threshold, and it is suppressed when its field energy is above the threshold. These results explain why and how multiple firing modes are induced and controlled in biological neurons. Furthermore, the self-adaption property of memristive neurons was also clarified. Thus, the control of energy flow in the memristive synapse can effectively regulate the membrane potentials, and neural activities can be effectively controlled to select suitable body gaits.

memristive synapse, electromagnetic induction, neural circuit, Hamilton energy

Citation: Wu F Q, Guo Y T, Ma J. Energy flow accounts for the adaptive property of functional synapses. Sci China Tech Sci, 2023, 66: 3139–3152, https://doi.org/10.1007/s11431-023-2441-5

1 Introduction

memristors are important electric components that have potential applications in designing artificial neurons for reliable neuromorphic computing [1–5]. In circuit implementation [6,7], equivalent components are combined to mimic the functional characteristics of an ideal memristor; then, a memristive current is generated to control nonlinear circuits for developing the coexistence of multiple attractors and stabilizing multistability [8–10]. When a neural circuit is activated by a memristor-like element, the memristive channel is activated to encode the shunted current or couple the adjacent neural circuit as a memristive synapse [11–15]. As reported in refs. [16,17], memristive synapses can present similar synaptic plasticity when they are activated to regulate isolated neurons or connect more neurons in networks. The coupling channels exhibit practical controllability when the memristive synapse is used to couple neurons, and synchronous patterns can be effectively controlled [18,19]. Wu et al. [20] confirmed that a memristive synapse can express

*Corresponding author (email: hyperchaos@lut.edu.cn, hyperchaos@163.com)

biophysical functions similar to a chemical synapse, and a memristive current [21] can be effectively used to estimate the electromagnetic radiation (EMR) effect in biological neurons.

From the dynamical aspect, memristor-connected systems can be updated with some equivalent dynamical systems, in which the dynamical properties are dependent on the initial values of memristive variables by involving variable-dependent gains in the memristive terms, and any changes in the initial values will induce mode transition in the electrical activities [22–26]. As a result, the synchronization stability [27–30] is controlled by the coupling intensity and initials for memristive variables as well. For example, an EMR can induce resonance synchronization between memristive neurons without synaptic coupling because external energy can be encoded and absorbed in the memristive channel.

The most important contribution of connecting a memristor to a neural circuit is that a similar memristive term is introduced to approach the EMR effect, which is considered as additive induced current in the biological neurons because diffusive intracellular and extracellular ions can induce the spatial distribution of the electromagnetic field. Herein, a memristive neuron model is suggested, and the biophysical importance of memristive current in the Hindmarsh-Rose neuron, including an additive magnetic flux variable, is explained [31,32]. Furthermore, a similar memristive term is added to other neuron models for estimating similar EMR effects on electrical activities [33–38]. In particular, the effect of field coupling [39–43] is activated to regulate the synchronous firing patterns and stability in neural networks. Field coupling is considered a superposition of magnetic flux that can effectively control the collective behavior of clustered neurons and even completely suppress synaptic coupling.

In the case of biological neurons, intrinsic controllability enables the distinct self-adaptive ability to generate the appropriate firing patterns or realize mode selection in neural activities. For example, the auditory and visual neurons detect acoustic waves and visible lights within specific wave bands, and the potential mechanism of wave filtering is explained in refs. [44,45]. Furthermore, a similar scheme for wave filtering [46] is used to control the firing patterns in biological neurons. When neurons are excited by external stimuli from multiple channels, they select the firing mode induced by an external stimulus with energy density [47,48], even with noise disturbance. For building artificial neural circuits, specific electrical components are required to enhance the biophysical function and obtain biophysical neurons/sensors. For example, the connection to a photocell can enhance its sensitivity to perceive external illumination in the neural circuit [49,50], and the connection to a thermistor can make the output voltage dependent on the temperature, obtaining a temperature-sensitive neuron model [51–54]. As a result, the spatial patterns in the network comprising thermosensitive neurons [55,56] will be completely controlled by temperature. These electrical components with specific physical characteristics can be combined to build hybrid synapses [57–60] for connecting neural circuits, creating controllable coupling channels.

In the past decades, memristors, including discrete memristors, have been used to improve the memory properties of nonlinear circuits, and the dynamics and application of memristive systems to image encryption have been investigated [61–64]. Particularly, vibrational resonance [65] can be induced in memristive neurons and networks. Memristors show potential application in the design of artificial synapses for possible neuromorphological calculations [66–70]. In this study, a memristor is used to control a simple nonlinear circuit by adding a new branch circuit in parallel, which captures and shunts the energy among different electrical components. Energy flow is shunted in the memristive channel of this circuit, and adaptive laws are proposed to explain the controllability of the memristive synapse. The authors suggested that the intensity of the memristive synapse is suppressed when the channel energy is larger than a certain threshold; thus, the inner electric field energy saved in the cell membrane (i.e., the capacitor in the neural circuit) can be maintained at a high proportion in the total field energy. Therefore, continuous energy absorption from the external field can control the intrinsic properties of the memristive channel/synapse, and the memristive neuron becomes controllable because of its distinct self-adaptive ability. From a physical viewpoint, energy accommodation in the memristive channel induces possible shape deformation, and some inner physical parameters are changed to synchronously adjust the memristive current. Thus, energy is further shunted to modify the firing patterns in the neuron effectively.

2 Model and scheme

A memristor is a specific electrical component that builds a connection to two physical variables, such as magnetic flux and charge, and its involvement in nonlinear circuits can induce the coexistence of attractors and the occurrence of multistability in dynamics. For some neural circuits, the creation of an additive memristive channel can introduce a memristive synapse, and the effect of electromagnetic induction/radiation can be well estimated. From the physical aspect, energy is shunted in the memristor or memristive channel when an additive branch circuit is used to connect a nonlinear memristor-like element. As shown in Figure 1, a magnetic flux-controlled memristor (MFCM) is connected to a simple nonlinear circuit (capacitor-coupled inductor and resistor), and an external voltage source (V_S) is used as the signal source.

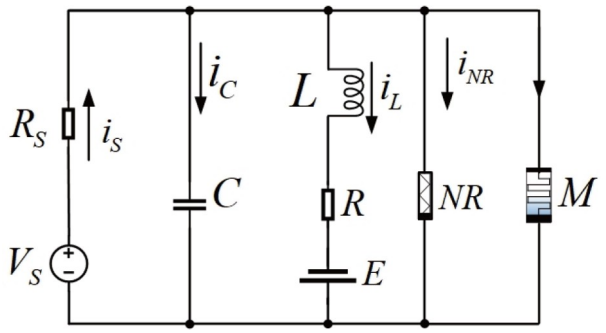

Figure 1 Schematic diagram of the memristive circuit coupled by a memristor (M). E is a constant voltage source.

The memristive current in the MFCM shown in Figure 1 is defined as follows:

$$i_M = \frac{\mathrm{d}q(\phi)}{\mathrm{d}\phi}\frac{\mathrm{d}\phi}{\mathrm{d}t} = M(\phi)V_M = k_M(\alpha + 3\beta\phi^2)V, \tag{1}$$

where V denotes the output voltage of the nonlinear resistor (NR), and C represents the capacitance of the capacitor. The gain (k_M) is dependent on the material property of the memristor, and it can capture energy in an equivalent inductor with N turns as $k_M = 1/N$. V_M is the average induced electromotive force for the memristor and is expressed as $k_M V$. The physical parameters α and β are independent of the magnetic flux (ϕ) across the channel. The channel current along NR shown in Figure 1 is calculated as follows [71]:

$$i_{NR} = -\frac{1}{\rho}\left(V - \frac{1}{3}\frac{V^3}{V_0^2}\right). \tag{2}$$

The physical parameters ρ and V_0 represent the constant resistance and cutoff voltage in the current-voltage (i-v) curve for the NR. The dynamics of the memristive circuits is calculated by

$$\begin{cases} C\dfrac{\mathrm{d}V}{\mathrm{d}t} = \dfrac{V_S - V}{R_s} - i_L - i_{NR} - i_M, \\ L\dfrac{\mathrm{d}i_L}{\mathrm{d}t} = V - Ri_L + E, \\ \dfrac{\mathrm{d}\phi}{\mathrm{d}t} = V_M + \phi_{\mathrm{ext}}. \end{cases} \tag{3}$$

The biophysical properties of the membrane, ion channel, and reverse potential of the neuron can be controlled by some physical parameters—C, L, E, R_S, and R. By controlling the external voltage source (V_S), the excitability can be adjusted, and the neural activities can be effectively regulated. ϕ_{ext} represents the external EMR. For better dynamical analysis, a couple of dimensionless coefficients and variables are defined as follows:

$$\begin{cases} x = \dfrac{V}{V_0}, y = \dfrac{\rho i_L}{V_0}, \tau = \dfrac{t}{\rho C}, a = \dfrac{E}{V_0}, b = \dfrac{R}{\rho}, \\ c = \dfrac{\rho^2 C}{L}, \varphi = \dfrac{\phi}{\rho C V_0}, \xi = \dfrac{\rho}{R_s}, \\ u_s = \dfrac{V_s \rho}{R_s V_0} = \xi\dfrac{V_s}{V_0}, \alpha' = \alpha\rho, \beta' = 3\beta\rho^3 C^2 V_0^2. \end{cases} \tag{4}$$

Additionally, the dynamics of a memristive neuron model under EMR are expressed as follows:

$$\begin{cases} \dfrac{\mathrm{d}x}{\mathrm{d}\tau} = x(1-\xi) - \dfrac{1}{3}x^3 - y + u_s - k_M(\alpha' + \beta'\varphi^2)x, \\ \dfrac{\mathrm{d}y}{\mathrm{d}\tau} = c(x + a - by), \\ \dfrac{\mathrm{d}\varphi}{\mathrm{d}\tau} = k_M x + \varphi_{\mathrm{ext}}, \end{cases} \tag{5}$$

where the variables x, y, and φ represent the membrane potential, channel current, and dimensionless magnetic flux, respectively. The normalized parameters a, b, c, and ξ can be controlled in the memristive neuron. The equivalent transmembrane current (u_s) can arise from a photocurrent or piezoelectric current and it can be adjusted to effectively control the memristive neuron. When EMR is applied, the isolated neuron will present various firing modes. Particularly, the coexistence of multiple firing modes can be induced because of the induction current across the memristive channel. The control mechanism of the self-adaptive ability of the memristive neuron is elucidated by discussing the energy in the electrical components (E_C for the capacitor, E_L for the inductor, and E_M for the memristor). Energy release controls the firing states in the memristive neuron.

$$\begin{cases} E_C = \dfrac{1}{2}CV^2, E_L = \dfrac{1}{2}Li_L^2, \\ E_M = \dfrac{1}{2}L_M i_M^2 = \dfrac{1}{2}\phi i_M = \dfrac{1}{2}k_M\phi(\alpha + 3\beta\phi^2)V, \\ E_{CLM} = E_C + E_L + E_M = \dfrac{1}{2}CV^2 + \dfrac{1}{2}Li_L^2 + \dfrac{1}{2}L_M i_M^2. \end{cases} \tag{6}$$

Thus, the dimensionless energy (H) of the memristive neuron can be effectively used to measure the physical characteristics of the memristive circuit controlled by energy flow.

$$\begin{cases} H = \dfrac{E_{CLM}}{CV_0^2} = \dfrac{1}{2}x^2 + \dfrac{1}{2c}y^2 + \dfrac{1}{2}k_M\alpha' x\varphi + \dfrac{1}{2}k_M\beta' x\varphi^3, \\ H_M = \dfrac{E_M}{CV_0^2} = \dfrac{1}{2}k_M(\alpha' x\varphi + \beta' x\varphi^3), \\ H_C = \dfrac{E_C}{CV_0^2} = \dfrac{1}{2}x^2, H_L = \dfrac{E_L}{CV_0^2} = \dfrac{1}{2c}y^2. \end{cases} \tag{7}$$

The last two terms in eq. (7) represent the consumed and saved energy in the memristive synapse. The third term of H can be considered as the Joule heat within one time unit in the memristor, and the last term defines the memristive field energy. Most electrical components can store field energy with certain saturation values, and continuous energy injection will induce energy overflow/release. The reliability of the Hamilton function in eq. (7) can be confirmed and expressed using the Helmholtz theorem [72,73] (see Appendix). The activation of self-adaption in the memristive synapse means that its parameters can be adjusted under special physical conditions. In the presence of continuous energy accommodation and injection, shape deformation in

media occurs, and some corresponding parameters are expressed as follows:

$$\frac{\mathrm{d}k_M}{\mathrm{d}\tau} = \sigma \cdot k_M \vartheta\left(\left|\frac{H_M}{H}\right| - \lambda\right),$$
$$\vartheta(P) = 1, P \geqslant 0, \vartheta(P) = 0, P < 0, \tag{8}$$

where the threshold (λ) controls the parameter shift during energy accommodation when the energy level in the memristive synapse is beyond the threshold ratio. The positive parameter (σ) can effectively increase the gain (k_M) for the memristive synapse and synaptic current. The field energy in the memristive synapse can have a negative value because the membrane potential can be negative, indicating that the memristive synapse behaves as an energy source to inject energy into other channels. Thus, the absolute value symbol |*| is applied to calculate the energy proportion of the neuron.

As described in eq. (8), parameter shift results from the media deformation due to energy absorption, and energy flow is shunted in different types/channels. To discern the energy dependence on firing patterns, the energy proportions (p_1, p_2, p_3) in different channels are calculated as follows:

$$p_1 = \frac{H_C}{H},$$
$$p_2 = \frac{H_L}{H}, \tag{9}$$
$$p_3 = \left|\frac{H_M}{H}\right|,$$

where absolute value calculation is applied to determine the energy proportion of the memristive synapse because its energy defined in eq. (7) can be negative during the change of membrane potential. Thus, p_3 can have values higher than 1 when neural activities are regulated.

3 Results and discussion

In this section, the fourth-order Runge-Kutta algorithm is applied to determine the exact numerical solutions with time step $h = 0.01$, and the parameters in eq. (5) are assigned the following values: $a = 0.7$, $b = 0.4$, $c = 1.0$, and $\xi = 0.175$. The external stimulus is selected with $u_s = 1 + \cos\omega\tau = 1 + \cos 2\pi k_M \tau$, $\alpha' = 0.1$, and $\beta' = 0.01$ for most cases. The memristive gain (k_M) is adjusted to trigger different firing patterns, as shown in Figure 2.

The results confirmed that four different firing modes, i.e., periodic, bursting, chaotic, and spiking activities, can be produced in the memristive neuron, indicating that the memristive channel can control mode selection in neural activities by controlling the memristive current and excitability of the neuron. A single firing mode is modulated to show multiple modes in neural activities at a high EMR intensity. Bifurcation analysis was conducted to predict the occurrence of chaotic patterns in memristive neurons, as shown in Figure 3.

The bifurcation analysis revealed that memristive modulation can induce distinct mode transition in the firing mode, and the memristive current can effectively control neural activities. The energy characteristics of each type of

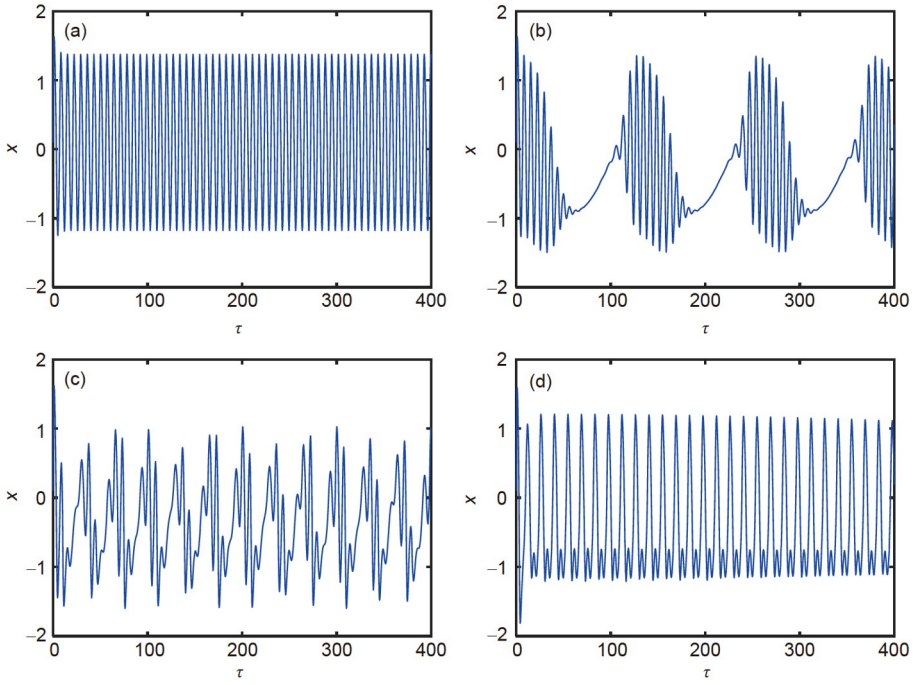

Figure 2 (Color online) Firing patterns for membrane potential are calculated by applying k_M = 0, 0.008, 0.03, 0.07. (a) Periodic firing; (b) bursting; (c) chaotic firing; (d) spiking pattern.

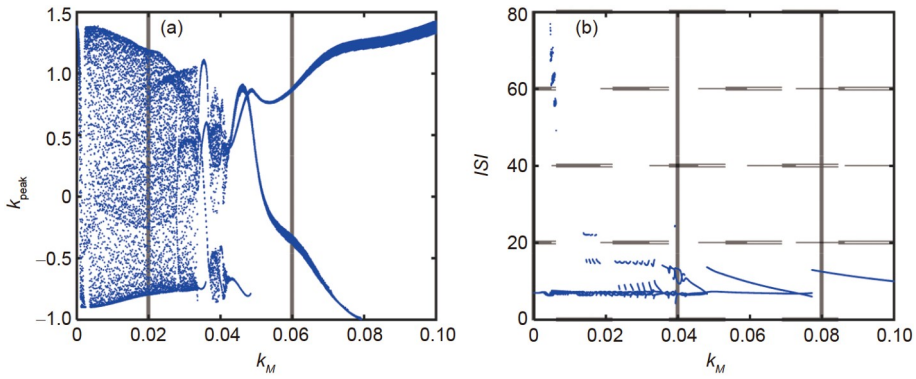

Figure 3 (Color online) Bifurcation diagram obtained by detecting the (a) membrane potential and (b) interspike interval with different gains (k_M). x_{peak} represents the peak value in the sampled time series for membrane potentials.

firing mode in an isolated neuron are determined, and the energy values of neurons exhibiting different patterns are estimated, as shown in Figure 4.

As shown in Figure 4a, the neuron exhibits a periodic pattern without memristive driving in the absence of the memristive current. In bursting neurons, the energy proportion for the memristive channel is small and negative energy occurs intermittently. In chaotic neurons, the memristive channel maintains a low energy proportion. In spiking neurons, energy is shunted in the memristive channel to maintain a high energy proportion for the capacitive and inductive channels. Furthermore, external EMR with a noisy type (Gaussian white noise with intensity D, zero average $<\varphi_{ext}> = 0$, $<\varphi_{ext}(\tau)\ \varphi_{ext}(\tau')>= 2D\delta(\tau-\tau')$, and $\delta(*)$ denoting the Dirac-δ function) is considered, and the gain for the memristive channel is fixed at $k_M = 0.008$. Then, the energy and membrane potential are calculated by applying different EMR intensities, as shown in Figure 5.

With further increases in the EMR intensity, the firing mode (bursting patterns) and energy value of the memristive neuron considerably change because of distinct changes in the memristive current and excitability. Importantly, bursting patterns are regulated to achieve multiple firing modes when the memristive synapse continues to capture energy at a high EMR intensity. The case of another gain, $k_M = 0.03$, is illustrated in Figure 6.

It is confirmed that chaotic patterns can be suppressed, in Figure 6, and the Hamilton energy in the memristive neuron is considerably increased when the EMR intensity is further increased. Indeed, more field energy is injected and absorbed in the neuron. Chaotic neurons often have a low Hamilton energy, and the occurrence of spiking will keep higher en-

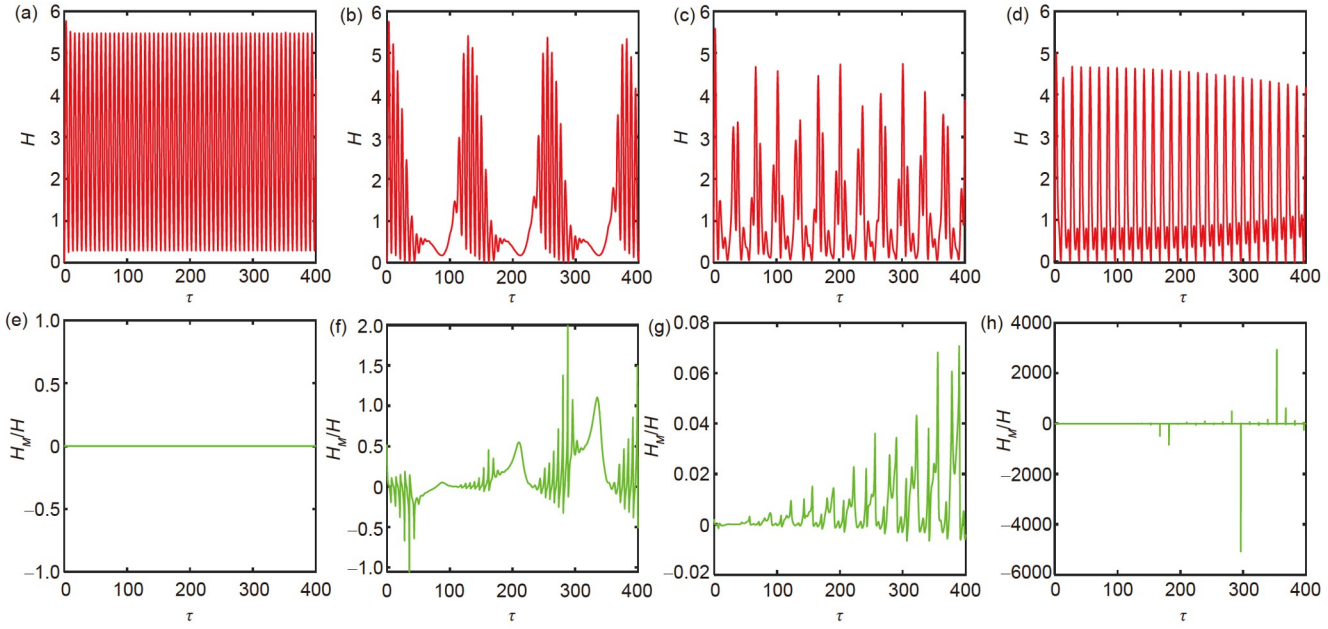

Figure 4 (Color online) Evolution of the Hamilton energy and memristive energy ratio of a memristive neuron. (a), (e) Periodic neuron, $k_M = 0$; (b), (f) bursting neuron, k_M =0.008; (c), (g) chaotic neuron, k_M =0.03; (d), (h) spiking neuron, $k_M = 0.07$.

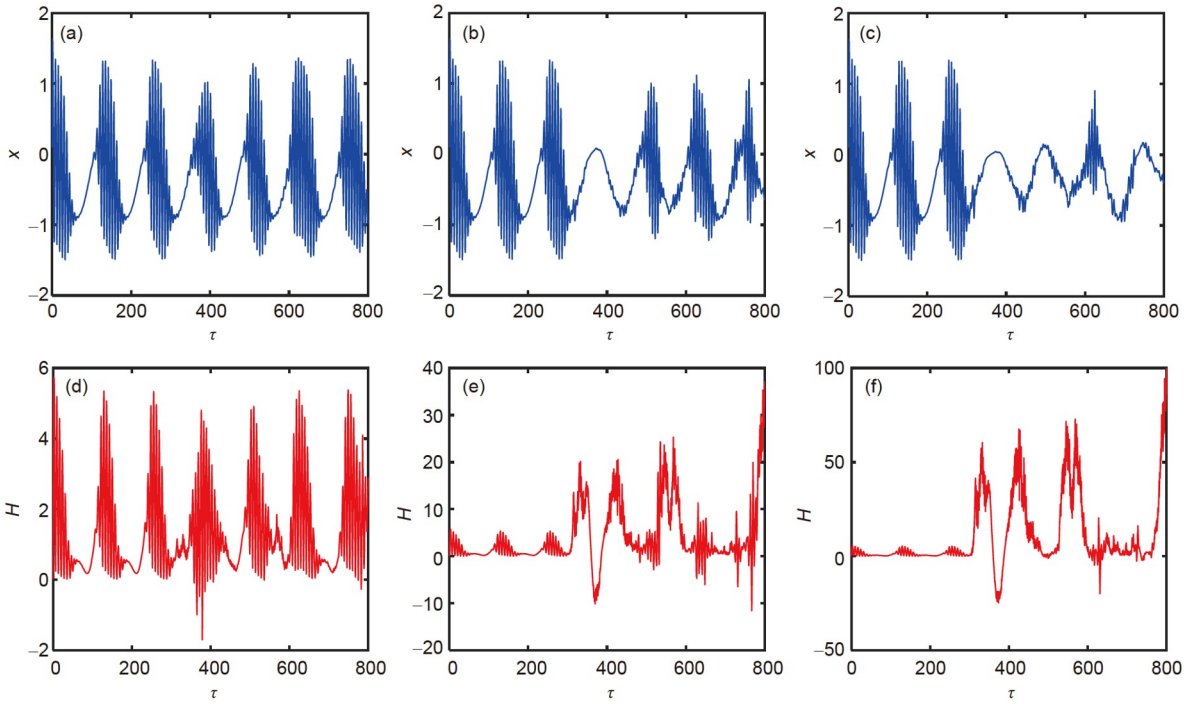

Figure 5 (Color online) (a)–(c) Sampled membrane potential x at D = 20, 60, 100 and k_M = 0.008; (d)–(f) evolution of energy function H at noise intensity D = 20, 60, 100 and k_M = 0.008. Noisy EMR is activated on the neuron at τ = 300 time units.

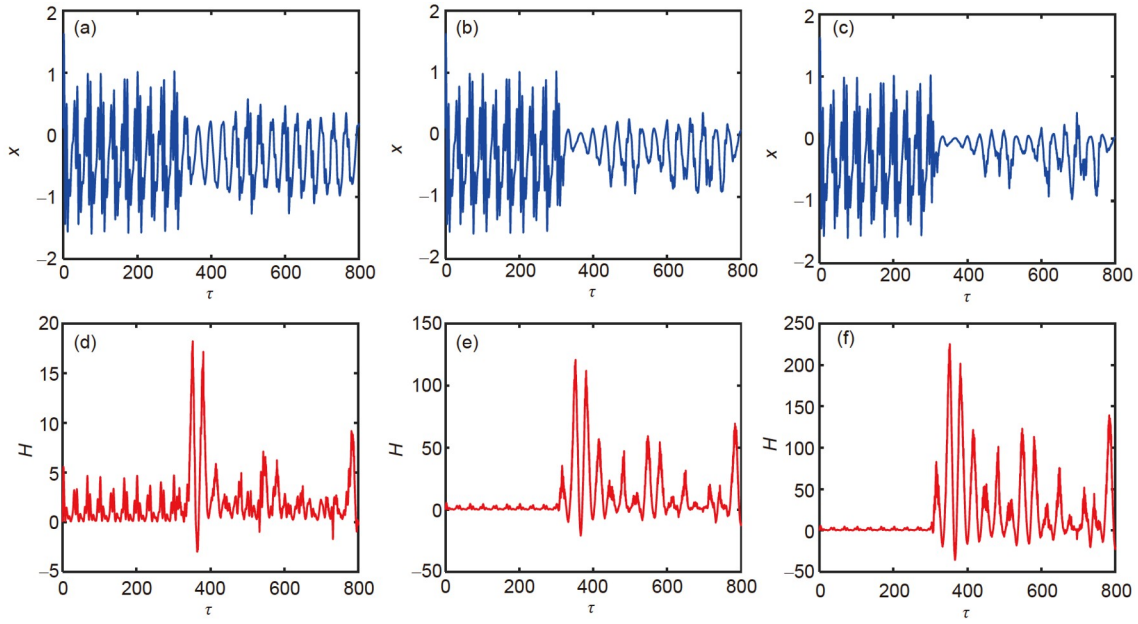

Figure 6 (Color online) (a)–(c) Sampled membrane potential x at noise intensity D = 20, 60, 100 and k_M = 0.03; (d)–(f) evolution of energy function H at noise intensity D = 20, 60, 100 and k_M = 0.03. Noisy EMR is activated on the neuron at τ = 300 time units.

ergy in the neuron, as a result, the enhancement of EMR will induce detectable mode transition in the memristive neuron. That is, the activation of memristive neurons can enhance the energy-keeping capability, and energy is released to adaptively regulate the neural activities.

According to eq. (7), the Hamilton energy contains three parts, i.e., the electric field energy (H_C), magnetic field energy (H_L), and channel energy (magnetic field energy, H_M), in the memristive channel. The memristive synapse can easily detect the effect of external stimuli. Thus, energy growth in the memristive channel, when the memristive neuron is controlled to achieve different firing patterns, needs to be investigated (Figure 7).

Figure 7 indicates that higher value for the memristive gain

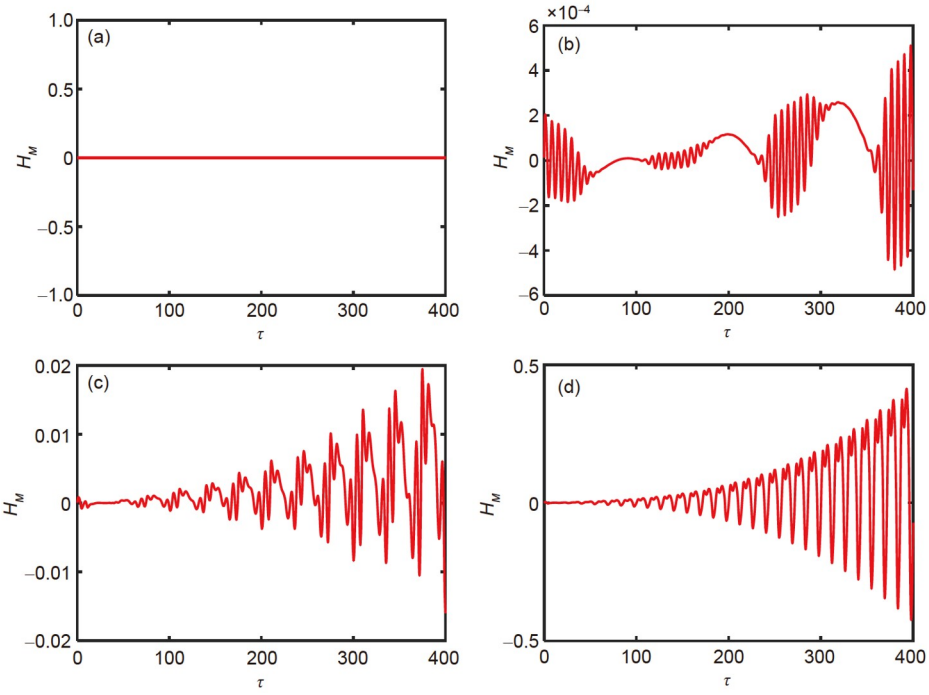

Figure 7 (Color online) Energy evolution in the memristive channel. For (a) $k_M = 0$ (periodic neuron); (b) $k_M = 0.008$ (bursting neuron); (c) $k_M = 0.03$ (chaotic neuron); (d) $k_M = 0.07$ (spiking neuron). The parameters are fixed at $a = 0.7$, $b = 0.4$, $c = 1.0$, $\xi = 0.175$, and the external stimulus is selected with $u_s = 1 + \cos 2\pi k_M \tau$.

(k_M) can increase the energy value of the memristive synapse. Thus, energy flow in the memristive neuron is shunted to slow down the firing patterns, and neural activities are completely controlled. According to eq. (9), the energy proportion is determined, as shown in Figure 8.

The neural activities exhibit distinct periodic oscillation in the absence of energy shunting from memristive synapse. With the increase in the memristive gain value, the memristive current is enhanced, and the energy proportion (p_3) is beyond 1 for the spiking neuron because the memristive channel presents a negative value for channel energy. In chaotic neurons, all of the energy proportions change within 0–1, and the average value of magnetic field energy is lower than that of the electric field energy. In periodic and spiking neurons, the magnetic field energy often exhibits a higher value compared to the electric field energy.

From the physical viewpoint, continuous absorption of external energy can change the physical properties of the memristor; furthermore, the gain of the memristive channel will be adjusted, as expressed in eq. (8), from a low k_M value of 0.001 at $\tau = 0$. That is, the propagated energy in the memristive synapse will adjust the energy flow in other channels and electrical components, and the activation of EMR will inject more energy into the neuron. For simplicity, the EMR is imposed at $\tau = 0$, and the memristive channel/synapse is synchronously regulated. The mode transition in neural activities is plotted in Figures 9 and 10.

At a low EMR intensity at $D = 10$, $\lambda = 0$ means that the gain of the memristive synapse continuously increases, and the memristive regulation is further enhanced to change the bursting intervals. Furthermore, the gain of the memristive synapse continuously increases without reaching saturation when the bursting patterns are regulated by the memristive current. On the other hand, when the threshold for growth in the memristive channel is high, the gain of the memristive synapse will slightly shift close to the constant value, indicating that the shunted energy in the memristive channel can be lower than the total energy value of neurons. Otherwise, the gain of the memristive synapse will rapidly increase. The extensive numerical results confirmed that the gain (k_M) of the memristive synapse continuously increases until it reaches a certain saturation value. That is, the growth of the memristive gain becomes intermittent because energy flow across the memristive channel is switched with the firing modes.

A low EMR intensity induces regular firing patterns than multiple modes in the firing patterns; however, the memristive synapse can effectively control the bursting patterns. When the threshold (λ) has a high value, the memristive channel can activate its growth only when high energy is shunted in the memristive channel. Otherwise, the memristive current cannot effectively hinder external stimuli (u_s), and the excitability and firing patterns are mainly controlled by external stimuli. Furthermore, the EMR is enhanced, and the self-adaptive ability of the memristive synapse is estimated, as shown in Figure 10.

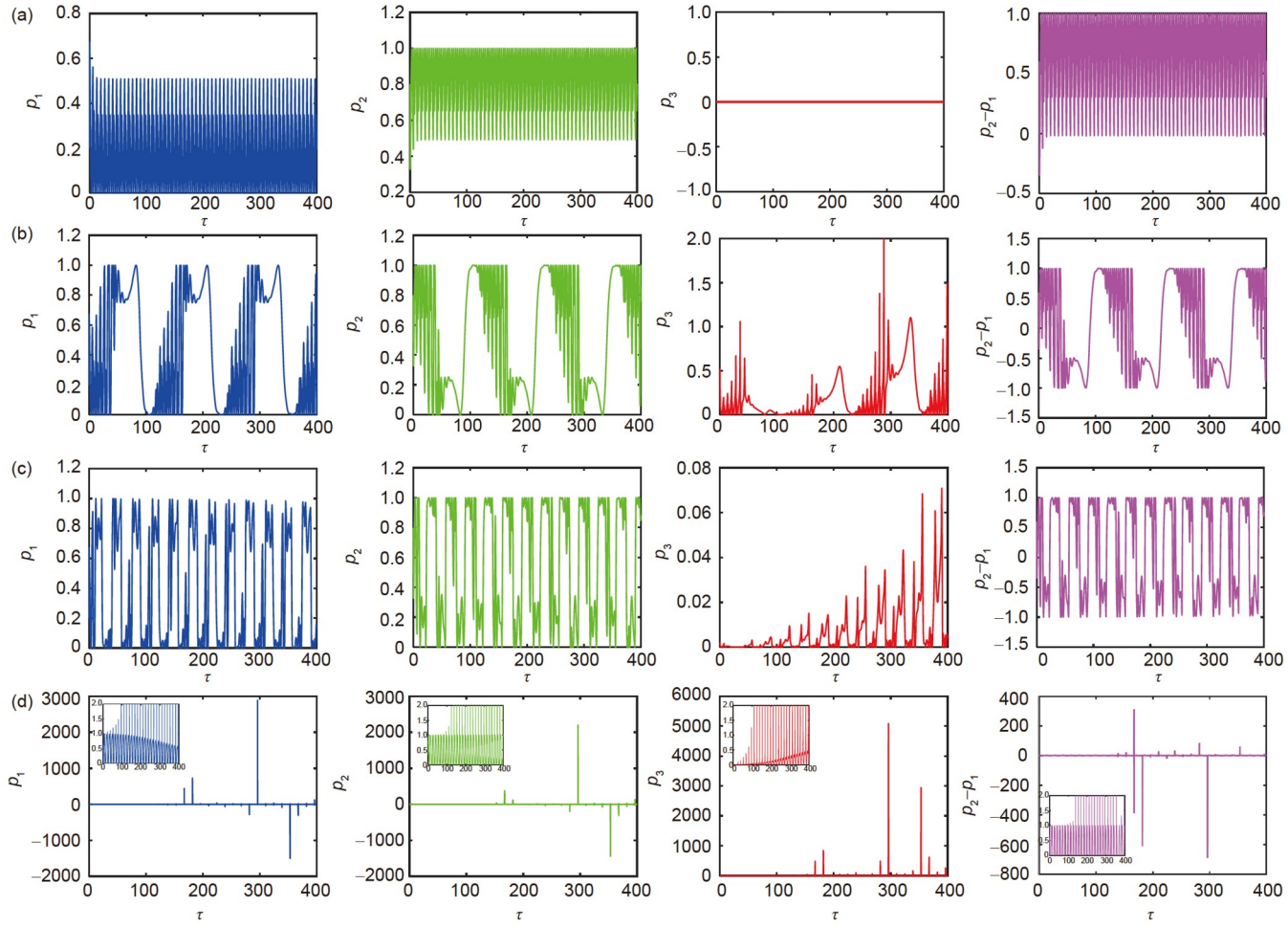

Figure 8 (Color online) Evolution of energy proportion in the memristive neuron. (a) $k_M = 0$ (periodic neuron); (b) $k_M = 0.008$ (bursting neuron); (c) $k_M = 0.03$ (chaotic neuron); (d) $k_M = 0.07$ (spiking neuron). The parameters are fixed at $a = 0.7$, $b = 0.4$, $c = 1.0$, and $\xi = 0.175$, and the external stimulus is selected with $u_s = 1 + \cos 2\pi k_M \tau$. The inset figures are enlarged versions.

When a neuron is exposed to a high-intensity EMR, the memristive channel can capture more energy, and the modulation of the memristive current will be considerably enhanced. The neural activities also exhibit multiple modes. As shown in Figure 10, at a low threshold in eq. (8) with zero value for λ, the memristive synapse controls the neural activities effectively by activating a strong memristive current. By applying a high threshold for λ, the gain of the memristive synapse will increase when its inner energy has a high proportion of the total energy (H). After a transient period, the memristive gain (k_M) will reach a saturation value and neural activities are suppressed to a quiescent state. The higher the value of threshold (λ), the higher the saturation value of the memristive gain (k_M). Particularly, the Hamilton energy (H) has a negative value when EMR is imposed on the neuron because the memristive channel captures more energy and becomes a continuous energy source with a negative value, which has a higher absolute value than the energy saved in other channels. When the EMR intensity is further increased, the memristive neuron will present multiple modes of electrical activities, and stable energy absorption will induce a change in energy flow along the memristive channel. When the energy value is beyond a certain threshold, the memristive synapse has to shape its profile, and some controllable parameters are adjusted to shunt the energy flow. As a result, the self-adaption property enables controllability under external energy injection. Thus, the memristive neuron exhibits more flexibility and reliability in signal processing and information encoding. Particularly, the memristive synapse under the proposed adaptive criterion enables controllability in multiple modes in neural activities.

As mentioned previously, the frequency of the external stimulus is relative to the memristive gain (k_M) because realistic external forcing signals are often filtered and encoded by the media. That is, the equivalent transmembrane current (u_s) will maintain a certain frequency band; thus, the gain (k_M) is introduced to the forcing current (u_s). For better contrast, $u_s = 1 + \cos 2\pi f\tau$ is imposed, and the appropriate memristive gain (k_M) is selected to investigate the developed patterns, as shown in Figure 11.

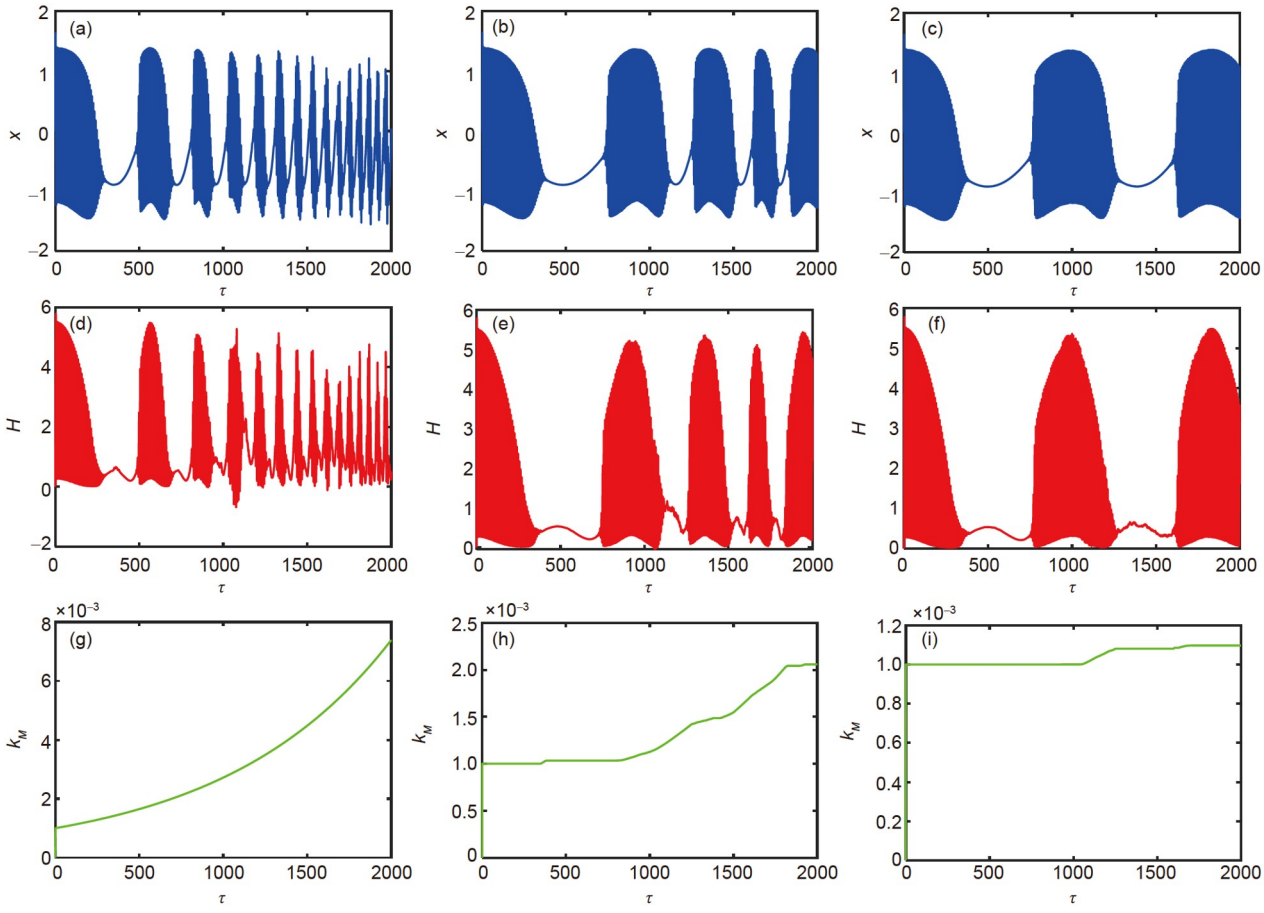

Figure 9 (Color online) (a)–(c) Sampled membrane potential x; (d)–(f) evolution of energy function H; (g)–(i) growth of the gain (k_M) of the memristive synapse under EMR. EMR is activated on the neuron at $\tau = 0$ time unit, and the parameters are fixed at noise intensity $D = 10$, $a = 0.7$, $b = 0.4$, $c = 1.0$, $\xi = 0.175$, $\sigma = 0.001$, and $\lambda = 0.0$, 0.1, 0.4.

By applying a higher gain to the memristive synapse, the bursting neuron is suppressed to achieve distinct periodic oscillation in the neural activities, and the firing mode is effectively suppressed. According to eq. (8), energy flow in the memristive channel can control the energy shunting and firing modes. The capacitor and inductor can also capture energy from the external electric and magnetic fields. Thus, continuous energy absorption from the capacitive and inductive fields can also induce a certain shape deformation, which is expressed using parameter shift in eq. (10).

$$\begin{cases} \dfrac{\mathrm{d}k_M}{\mathrm{d}\tau} = \sigma \cdot k_M \vartheta\left(\dfrac{H_C}{H} - \lambda\right) = \sigma \cdot k_M \vartheta(p_1 - \lambda), \\ \vartheta(P) = 1, P \geqslant 0, \vartheta(P) = 0, P < 0, \\ \dfrac{\mathrm{d}k_M}{\mathrm{d}\tau} = \sigma \cdot k_M \vartheta\left(\dfrac{H_L}{H} - \lambda\right) = \sigma \cdot k_M \vartheta(p_2 - \lambda), \\ \vartheta(P) = 1, P \geqslant 0, \vartheta(P) = 0, P < 0. \end{cases} \tag{10}$$

That is, continuous energy injection and absorption into the capacitive and inductive channels can enhance energy shunting and exchange between different channels. Furthermore, the memristive channel may share more energy and possible shape deformation can be induced. As shown in Figure 12, external radiation is applied to inject energy into the neuron, and the firing patterns are plotted to estimate the effects of shape deformation and parameter shift.

As shown in Figure 12, any changes in p_1 and p_2 can adjust the energy proportion (p_3), and then the memristive channel is shaped to adjust its gain (k_M). In a long transient period, the memristive synapse current will stabilize the firing patterns. Theoretically, the memristive gain can be increased to a certain saturation value, and neural activities can be suppressed. The energy flow is shunted to adjacent neurons in the neural network and functional regions of the nervous system. Thus, the memristive channel increases its gain intermittently rather than rapidly reaching saturation value to terminate the firing activities in the neuron. Moreover, energy flow can be controlled by enhancing the memristive synapse function, and synchronous bursting among neurons can be blocked to prevent seizures.

In realistic materials, the media may present diamagnetic or paramagnetic properties under an external magnetic field. For biological neurons, the media may exhibit different biophysical properties under EMR. As shown in Figure 1, the memristive channel shunts current from the external voltage source and the memristive current is mapped into the dimensionless form $k_M(\alpha + \beta\varphi^2)x$, and the gain ($k_M$) is

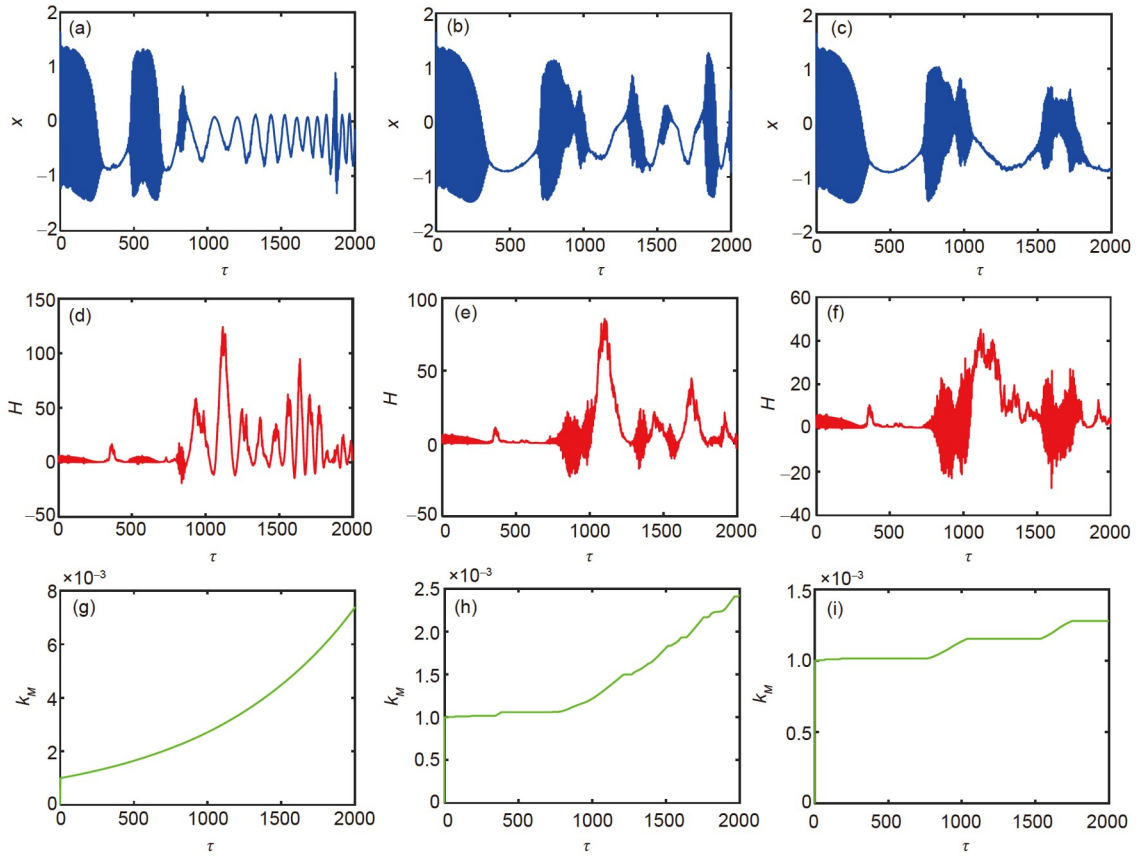

Figure 10 (Color online) (a)–(c) Sampled membrane potential x; (d)–(f) evolution of energy function H; (g)–(i) growth of the gain (k_M) of the memristive synapse under EMR. Noisy EMR is activated on the neuron at $\tau = 0$ time units, and noise intensity $D = 50$, $a = 0.7$, $b = 0.4$, $c = 1.0$, $\xi = 0.175$, $\sigma = 0.001$, and $\lambda = 0.0$, 0.9, 1.0.

considered to be a positive value that further increases with energy flow under EMR. Excitability is mainly controlled by the external stimulus (u_s). In the presence of EMR, continuous energy injection will make the memristive synapse shunt energy as the signal source and it is effective to keep against the excitation from u_s. Thus, from the dynamical aspect, the gain (k_M) of the memristive synapse can decrease its positive initial value. For simplicity, our scheme is implemented on a simple neural circuit by incorporating a memristor in an additive branch circuit to generate a memristive current that matches the effect of electromagnetic induction (EMI). The field energy is accurately defined and is consistent with the equivalent form obtained using the Helmholtz theorem. A similar scheme can be used for the biophysical neuron models considering more physical effects under EMR.

In the past decades, extensive studies have been conducted to understand the adaptive function in biological neurons by explaining the synaptic plasticity, controllability of ion channels, and functional regulation of astrocytes in synaptic connections in neural networks [41,74–77]. In particular, appropriate terms such as memristive current are introduced into the neuron models to estimate the effects of EMI and EMR, and the functional role of energy flow is discussed. Most biological neurons are flexible, and continuous energy accommodation may induce shape deformation accompanied by certain changes in physical parameters, including membrane capacitance, ion channel conductance, and reverse potential. As a result, some normalized parameters in the neuron model will change under continuous injection of energy flow. From the physical viewpoint, shape deformation in the capacitor or induction coil will change their energy storage and physical parameters in the presence of the electromagnetic field. The intrinsic parameters of the biological media will change under energy radiation, and this characteristic can be described by parameter shifts in the theoretical models. Our scheme aims to explain the physical mechanism of self-adaption in neurons under energy flow. The appropriate regulation of energy will control the firing mode in a single neuron and ensure cooperation between more neurons in the network. For further guidance, please refer to recent review papers and references therein [78,79].

4 Conclusions

Herein, a memristor-coupled neural circuit is proposed, and the memristive channel is used to estimate the effect of

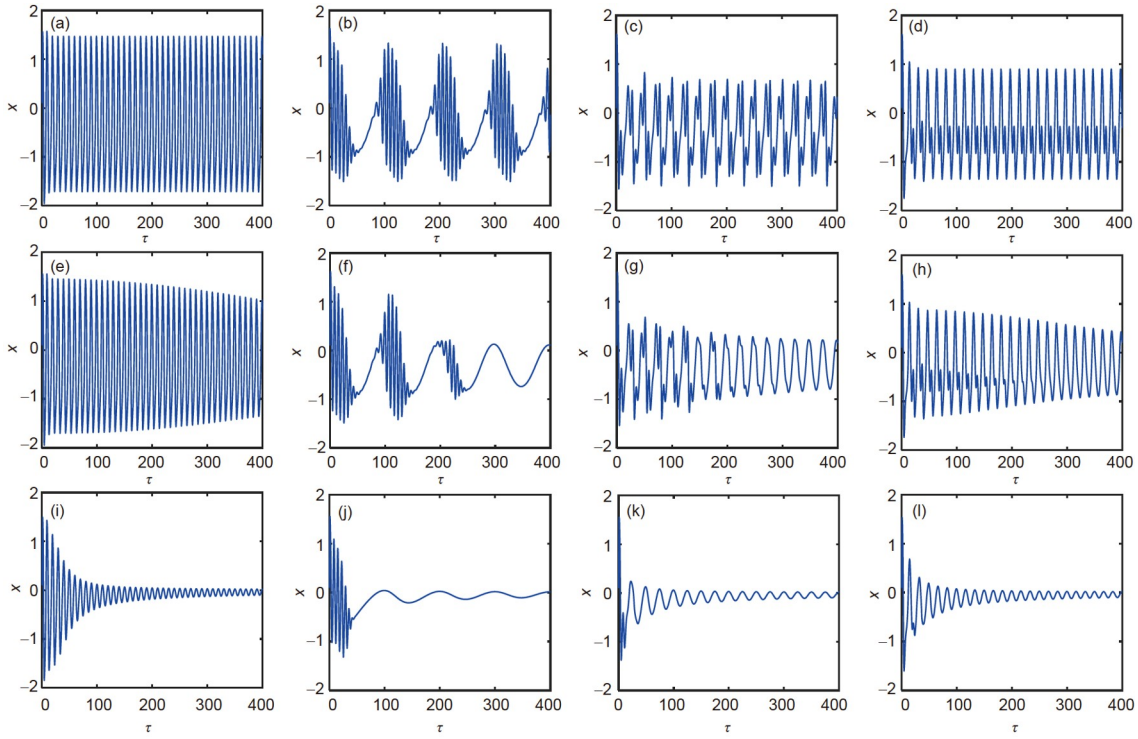

Figure 11 (Color online) Evolution of membrane potential under different memristive currents and external stimuli. (a) $f = 0.1$, $k_M = 0.01$; (b) $f = 0.01$, $k_M = 0.01$; (c) $f = 0.04$, $k_M = 0.01$; (d) $f = 0.06$, $k_M = 0.01$; (e) $f = 0.1$, $k_M = 0.15$; (f) $f = 0.01$, $k_M = 0.15$; (g) $f = 0.04$, $k_M = 0.15$; (h) $f = 0.06$, $k_M = 0.15$; (i) $f = 0.1$, $k_M = 1$; (j) $f = 0.01$, $k_M = 1$; (k) $f = 0.04$, $k_M = 1$; (l) $f = 0.06$, $k_M = 1$.

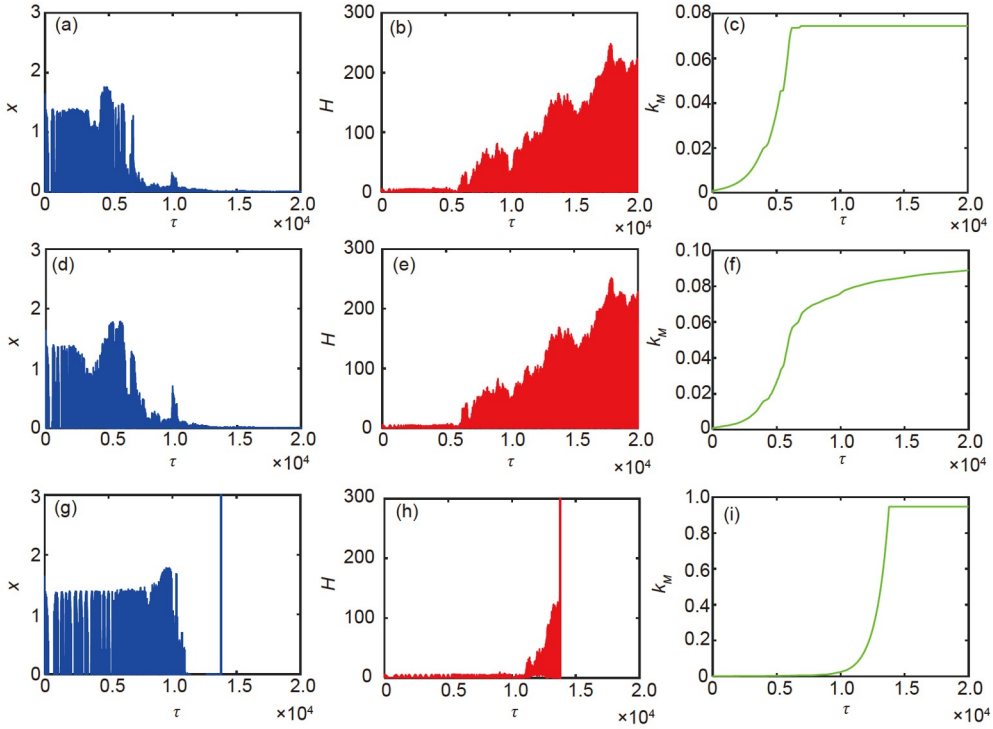

Figure 12 (Color online) Firing patterns, Hamilton energy, and memristive gain (k_M) in the presence of noisy radiation. (a)–(c) k_M controlled by p_1; (d)–(f) k_M controlled by p_2; (g)–(i) k_M controlled by p_3. Setting $D = 10$, $a = 0.7$, $b = 0.4$, $c = 1.0$, $\xi = 0.175$, $\sigma = 0.001$, and $\lambda = 0.1$.

electromagnetic induction in biological neurons during the diffusive propagation of intracellular and extracellular ions. A memristive neuron model is obtained to discern the effects of EMI and EMR, and the equivalent energy function for

isolated memristive neurons is confirmed in two ways. For the memristive neural circuit excited by an MFCM, the memristive channel consumes Joule heat and stores magnetic field energy. For the charge-controlled memristor, the memristive channel stores electric field energy and consumes Joule heat. When the EMR is enhanced, the memristive channel captures and absorbs more energy. As a result, the intrinsic physical properties are changed by adaptively adjusting the normalized parameters because of the strong magnetization resulting from EMR. We proposed an adaptive growth criterion for the normalized parameters in the memristive channel when more energy from the magnetic field is accumulated to induce shape deformation in the component. The membrane potential and Hamilton energy were calculated to reveal the mode transition and shift in energy when the memristive synapse is enhanced. Our results provide insights into the biophysical mechanism of adaptive growth and regulation in the memristive synapse. It also suggests that energy injection can be an effective way to control the neural activities of a single neuron and collective activities in neural networks. Moreover, this scheme can be effectively used to solve similar problems in a biophysical neuron excited by a noisy electric field [80]. For more guidance in this field, please refer to the suggestions and comments in a recent review [81].

Appendix

According to the Helmholtz theorem, the memristive neuron can be expressed in vector form as follows:

$$\begin{aligned}
\begin{pmatrix}\dot{x}\\ \dot{y}\\ \dot{\varphi}\end{pmatrix} &= \begin{pmatrix}x(1-\xi)-\frac{1}{3}x^3-y+u_s-k_M(\alpha'+\beta'\varphi^2)x\\ c(x+a-by)\\ k_M x\end{pmatrix} = F_c+F_d\\
&= \begin{pmatrix}-y-\frac{3}{2}k_M^2\beta'\varphi^2 x-\frac{1}{2}k_M^2\alpha' x\\ cx\\ k_M x+\frac{1}{2}k_M^2\beta'\varphi^3+\frac{1}{2}k_M^2\alpha'\varphi+\frac{y\varphi(\beta'\varphi^2+\alpha')}{x(3\beta'\varphi^2+\alpha')}\end{pmatrix}+\begin{pmatrix}x(1-\xi)-\frac{1}{3}x^3+u_s-k_M(\alpha'+\beta'\varphi^2)x+\frac{3}{2}k_M^2\beta'\varphi^2 x+\frac{1}{2}k_M^2\alpha' x\\ c(a-by)\\ -\frac{1}{2}k_M^2\beta'\varphi^3-\frac{1}{2}k_M^2\alpha'\varphi-\frac{y\varphi(\beta'\varphi^2+\alpha')}{x(3\beta'\varphi^2+\alpha')}\end{pmatrix}\\
&= \begin{pmatrix}0 & -c & -k_M\\ c & 0 & -\frac{c\varphi(\beta'\varphi^2+\alpha')}{x(3\beta'\varphi^2+\alpha')}\\ k_M & \frac{c\varphi(\beta'\varphi^2+\alpha')}{x(3\beta'\varphi^2+\alpha')} & 0\end{pmatrix}\begin{pmatrix}x+\frac{1}{2}k_M\alpha'\varphi+\frac{1}{2}k_M\beta'\varphi^3\\ \frac{y}{c}\\ \frac{1}{2}k_M\alpha' x+\frac{3}{2}k_M\beta' x\varphi^2\end{pmatrix}\\
&\quad+\begin{pmatrix}a_{11} & 0 & 0\\ 0 & c^2(\frac{a}{y}-b) & 0\\ 0 & 0 & a_{33}\end{pmatrix}\begin{pmatrix}x+\frac{1}{2}k_M\alpha'\varphi+\frac{1}{2}k_M\beta'\varphi^3\\ \frac{y}{c}\\ \frac{1}{2}k_M\alpha' x+\frac{3}{2}k_M\beta' x\varphi^2\end{pmatrix},
\end{aligned} \tag{A1}$$

$$\begin{cases}
a_{11}=\dfrac{x(1-\xi)-\frac{1}{3}x^3+u_s-k_M(\alpha'+\beta'\varphi^2)x+\frac{3}{2}k_M^2\beta'\varphi^2 x}{x+\frac{1}{2}k_M\beta'\varphi^3+\frac{1}{2}k_M\alpha'\varphi},\\
a_{33}=\dfrac{-\frac{1}{2}k_M^2\beta'\varphi^3-\frac{1}{2}k_M^2\alpha'\varphi-\frac{y\varphi(\beta'\varphi^2+\alpha')}{x(3\beta'\varphi^2+\alpha')}}{\frac{1}{2}k_M\alpha' x+\frac{3}{2}k_M\beta' x\varphi^2}.
\end{cases} \tag{A2}$$

Based on the Helmholtz theorem [72,73], the energy function is restricted by

$$\begin{cases}\nabla\mathbf{H}^{\mathrm{T}}F_c=0,\\ \nabla\mathbf{H}^{\mathrm{T}}F_d=\dot{H}=\dfrac{\mathrm{d}H}{\mathrm{d}\tau}.\end{cases} \tag{A3}$$

This is further verified by

$$\begin{aligned}
0=\nabla\mathbf{H}^{\mathrm{T}}F_c=&\left(-y-\frac{3}{2}k_M^2\beta'\varphi^2 x-\frac{1}{2}k_M^2\alpha' x\right)\frac{\partial H}{\partial x}+cx\frac{\partial H}{\partial y}+\\
&\left(k_M x+\frac{1}{2}k_M^2\beta'\varphi^3+\frac{1}{2}k_M^2\alpha'\varphi+\frac{y\varphi(\beta'\varphi^2+\alpha')}{x(3\beta'\varphi^2+\alpha')}\right)\frac{\partial H}{\partial\varphi},
\end{aligned} \tag{A4}$$

$$H=\frac{1}{2}x^2+\frac{1}{2c}y^2+\frac{1}{2}k_M\alpha' x\varphi+\frac{1}{2}k_M\beta' x\varphi^3. \tag{A5}$$

This work was supported by the National Natural Science Foundation of China (Grant No. 12072139).

1 Wang T, Shi Y, Puglisi F M, et al. Electroforming in metal-oxide memristive synapses. ACS Appl Mater Interfaces, 2020, 12: 11806–11814

2 Wang J, Zhuge F. Memristive synapses for brain-inspired computing.

Adv Mater Technol, 2019, 4: 1800544
3 Jang B C, Kim S, Yang S Y, et al. Polymer analog memristive synapse with atomic-scale conductive filament for flexible neuromorphic computing system. Nano Lett, 2019, 19: 839–849
4 Yang R, Huang H M, Guo X. Memristive synapses and neurons for bioinspired computing. Adv Electron Mater, 2019, 5: 1900287
5 Covi E, Brivio S, Serb A, et al. Analog memristive synapse in spiking networks implementing unsupervised learning. Front Neurosci, 2016, 10: 482
6 Long K, Zhang X. Memristive-synapse spiking neural networks based on single-electron transistors. J Comput Electron, 2020, 19: 435–450
7 Bao B C, Zhu Y X, Ma J, et al. Memristive neuron model with an adapting synapse and its hardware experiments. Sci China Tech Sci, 2021, 64: 1107–1117
8 Tabekoueng Z N, Shankar Muni S, Fonzin Fozin T, et al. Coexistence of infinitely many patterns and their control in heterogeneous coupled neurons through a multistable memristive synapse. Chaos, 2022, 32: 053114
9 Lin H, Wang C, Sun Y, et al. Firing multistability in a locally active memristive neuron model. Nonlinear Dyn, 2020, 100: 3667–3683
10 Fossi J T, Deli V, Njitacke Z T, et al. Phase synchronization, extreme multistability and its control with selection of a desired pattern in hybrid coupled neurons via a memristive synapse. Nonlinear Dyn, 2022, 109: 925–942
11 Sung S H, Kim T J, Shin H, et al. Simultaneous emulation of synaptic and intrinsic plasticity using a memristive synapse. Nat Commun, 2022, 13: 2811
12 Li R, Wang Z, Dong E. A new locally active memristive synapse-coupled neuron model. Nonlinear Dyn, 2021, 104: 4459–4475
13 Serb A, Corna A, George R, et al. Memristive synapses connect brain and silicon spiking neurons. Sci Rep, 2020, 10: 2590
14 Zhang Y, He W, Wu Y, et al. Highly compact artificial memristive neuron with low energy consumption. Small, 2018, 14: 1802188
15 Wu F, Zhang Y, Zhang X. Regulating firing rates in a neural circuit by activating memristive synapse with magnetic coupling. Nonlinear Dyn, 2019, 98: 971–984
16 Baran A Y, Korkmaz N, Öztürk I, et al. On addressing the similarities between STDP concept and synaptic/memristive coupled neurons by realizing of the memristive synapse based HR neurons. Eng Sci Tech Int J, 2022, 32: 101062
17 Lin H, Wang C, Deng Q, et al. Review on chaotic dynamics of memristive neuron and neural network. Nonlinear Dyn, 2021, 106: 959–973
18 Xu F, Zhang J, Fang T, et al. Synchronous dynamics in neural system coupled with memristive synapse. Nonlinear Dyn, 2018, 92: 1395–1402
19 Guo Y, Zhu Z, Wang C, et al. Coupling synchronization between photoelectric neurons by using memristive synapse. Optik, 2020, 218: 164993
20 Wu F, Guo Y, Ma J. Reproduce the biophysical function of chemical synapse by using a memristive synapse. Nonlinear Dyn, 2022, 109: 2063–2084
21 Wu F, Hu X, Ma J. Estimation of the effect of magnetic field on a memristive neuron. Appl Math Comput, 2022, 432: 127366
22 Chen M, Feng Y, Bao H, et al. State variable mapping method for studying initial-dependent dynamics in memristive hyper-jerk system with line equilibrium. Chaos Solitons Fractals, 2018, 115: 313–324
23 Bao H, Chen M, Wu H G, et al. Memristor initial-boosted coexisting plane bifurcations and its extreme multi-stability reconstitution in two-memristor-based dynamical system. Sci China Tech Sci, 2020, 63: 603–613
24 Zhang Y, Liu Z, Wu H, et al. Extreme multistability in memristive hyper-jerk system and stability mechanism analysis using dimensionality reduction model. Eur Phys J Spec Top, 2019, 228: 1995–2009
25 Wu H G, Ye Y, Bao B C, et al. Memristor initial boosting behaviors in a two-memristor-based hyperchaotic system. Chaos Solitons Fractals, 2019, 121: 178–185
26 Wu F, Ma J, Ren G. Synchronization stability between initial-dependent oscillators with periodical and chaotic oscillation. J Zhejiang Univ Sci A, 2018, 19: 889–903
27 Ma J, Xu W, Zhou P, et al. Synchronization between memristive and initial-dependent oscillators driven by noise. Physica A, 2019, 536: 122598
28 Huang P, Guo Y, Ren G, et al. Energy-induced resonance synchronization in neural circuits. Mod Phys Lett B, 2021, 35: 2150433
29 Ma J, Wu F, Wang C. Synchronization behaviors of coupled neurons under electromagnetic radiation. Int J Mod Phys B, 2017, 31: 1650251
30 Zhang Y, Zhou P, Yao Z, et al. Resonance synchronisation between memristive oscillators and network without variable coupling. Pramana, 2021, 95: 49
31 Ma J, Tang J. A review for dynamics of collective behaviors of network of neurons. Sci China Tech Sci, 2015, 58: 2038–2045
32 Lv M, Wang C, Ren G, et al. Model of electrical activity in a neuron under magnetic flow effect. Nonlinear Dyn, 2016, 85: 1479–1490
33 Xu Y, Jia Y, Ge M, et al. Effects of ion channel blocks on electrical activity of stochastic Hodgkin-Huxley neural network under electromagnetic induction. Neurocomputing, 2018, 283: 196–204
34 Wan Q, Yan Z, Li F, et al. Complex dynamics in a Hopfield neural network under electromagnetic induction and electromagnetic radiation. Chaos, 2022, 32: 073107
35 Takembo C N, Mvogo A, Fouda H P E, et al. Wave pattern stability of neurons coupled by memristive electromagnetic induction. Nonlinear Dyn, 2019, 96: 1083–1093
36 Yang Y, Ma J, Xu Y, et al. Energy dependence on discharge mode of Izhikevich neuron driven by external stimulus under electromagnetic induction. Cogn Neurodyn, 2021, 15: 265–277
37 Kafraj M S, Parastesh F, Jafari S. Firing patterns of an improved Izhikevich neuron model under the effect of electromagnetic induction and noise. Chaos Solitons Fractals, 2020, 137: 109782
38 Jin W Y, Wang A, Ma J, et al. Effects of electromagnetic induction and noise on the regulation of sleep wake cycle. Sci China Tech Sci, 2019, 62: 2113–2119
39 Yao Z, Wang C, Zhou P, et al. Regulating synchronous patterns in neurons and networks via field coupling. Commun Nonlinear Sci Numer Simul, 2021, 95: 105583
40 Wu F Q, Ma J, Zhang G. Energy estimation and coupling synchronization between biophysical neurons. Sci China Tech Sci, 2020, 63: 625–636
41 Zandi-Mehran N, Jafari S, Hashemi Golpayegani S M R, et al. Different synaptic connections evoke different firing patterns in neurons subject to an electromagnetic field. Nonlinear Dyn, 2020, 100: 1809–1824
42 Qin H, Wang C, Cai N, et al. Field coupling-induced pattern formation in two-layer neuronal network. Physica A, 2018, 501: 141–152
43 Ma S, Yao Z, Zhang Y, et al. Phase synchronization and lock between memristive circuits under field coupling. AEU-Int J Electron Commun, 2019, 105: 177–185
44 Guo Y, Zhou P, Yao Z, et al. Biophysical mechanism of signal encoding in an auditory neuron. Nonlinear Dyn, 2021, 105: 3603–3614
45 Zhang X, Ma J. Wave filtering and firing modes in a light-sensitive neural circuit. J Zhejiang Univ Sci A, 2021, 22: 707–720
46 Yu D, Wang G, Li T, et al. Filtering properties of Hodgkin-Huxley neuron on different time-scale signals. Commun Nonlinear Sci Numer Simul, 2023, 117: 106894
47 Xie Y, Ma J. How to discern external acoustic waves in a piezoelectric neuron under noise? J Biol Phys, 2022, 48: 339–353
48 Xie Y, Zhou P, Yao Z, et al. Response mechanism in a functional neuron under multiple stimuli. Physica A, 2022, 607: 128175
49 Xie Y, Yao Z, Hu X, et al. Enhance sensitivity to illumination and synchronization in light-dependent neurons. Chin Phys B, 2021, 30: 120510
50 Xie Y, Zhu Z G, Zhang X F, et al. Control of firing mode in nonlinear neuron circuit driven by photocurrent. Acta Phys Sin, 2021, 70:

210502
51 Liu Y, Xu W, Ma J, et al. A new photosensitive neuron model and its dynamics. Front Inform Technol Electron Eng, 2020, 21: 1387–1396
52 Guo Y, Wang C, Yao Z, et al. Desynchronization of thermosensitive neurons by using energy pumping. Physica A, 2022, 602: 127644
53 Xu Y, Ma J. Control of firing activities in thermosensitive neuron by activating excitatory autapse. Chin Phys B, 2021, 30: 100501
54 Tagne J F, Edima H C, Njitacke Z T, et al. Bifurcations analysis and experimental study of the dynamics of a thermosensitive neuron conducted simultaneously by photocurrent and thermistance. Eur Phys J Spec Top, 2022, 231: 993–1004
55 Hussain I, Ghosh D, Jafari S. Chimera states in a thermosensitive FitzHugh-Nagumo neuronal network. Appl Math Comput, 2021, 410: 126461
56 Xu Y, Ma J. Pattern formation in a thermosensitive neural network. Commun Nonlinear Sci Numer Simul, 2022, 111: 106426
57 Xie Y, Zhou P, Ma J. Energy balance and synchronization via inductive-coupling in functional neural circuits. Appl Math Model, 2023, 113: 175–187
58 Yao Z, Wang C. Collective behaviors in a multiple functional network with hybrid synapses. Physica A, 2022, 605: 127981
59 Yao Z, Wang C. Control the collective behaviors in a functional neural network. Chaos Solitons Fractals, 2021, 152: 111361
60 Zhang Y, Wang C N, Tang J, et al. Phase coupling synchronization of FHN neurons connected by a Josephson junction. Sci China Tech Sci, 2020, 63: 2328–2338
61 Sun J, Li C, Lu T, et al. A memristive chaotic system with hypermultistability and its application in image encryption. IEEE Access, 2020, 8: 139289–139298
62 Hu Y, Li Q, Ding D, et al. Multiple coexisting analysis of a fractional-order coupled memristive system and its application in image encryption. Chaos Solitons Fractals, 2021, 152: 111334
63 Tsafack N, Iliyasu A M, De Dieu N J, et al. A memristive RLC oscillator dynamics applied to image encryption. J Inf Security Appl, 2021, 61: 102944
64 Lai Q, Lai C, Zhang H, et al. Hidden coexisting hyperchaos of new memristive neuron model and its application in image encryption. Chaos Solitons Fractals, 2022, 158: 112017
65 Baysal V, Yilmaz E. Effects of electromagnetic induction on vibrational resonance in single neurons and neuronal networks. Physica A, 2020, 537: 122733
66 Mannan Z I, Adhikari S P, Yang C, et al. Memristive imitation of synaptic transmission and plasticity. IEEE Trans Neural Netw Learn Syst, 2019, 30: 3458–3470
67 Fang X, Tan Y, Zhang F, et al. Transient response and firing behaviors of memristive neuron circuit. Front Neurosci, 2022, 16: 922086
68 Ran Y, Pei Y, Zhou Z, et al. A review of Mott insulator in memristors: The materials, characteristics, applications for future computing systems and neuromorphic computing. Nano Res, 2023, 16: 1165–1182
69 Wang J, Cao G, Sun K, et al. Alloy electrode engineering in memristors for emulating the biological synapse. Nanoscale, 2022, 14: 1318–1326
70 Gao F, Chen Y, Li Y, et al. Investigation of electrical performance and synaptic long-term plasticity of memristive devices with new transition metal carbide. Semicond Sci Technol, 2020, 35: 035008
71 Kyprianidis I M, Papachristou V, Stouboulos I N, et al. Dynamics of coupled chaotic Bonhoeffer-van der Pol oscillators. WSEAS T Syst, 2012, 11: 516–526
72 Kobe D H. Helmholtz's theorem revisited. Am J Phys, 1986, 54: 552–554
73 Zhou P, Hu X, Zhu Z, et al. What is the most suitable Lyapunov function? Chaos Solitons Fractals, 2021, 150: 111154
74 Palabas T, Torres J J, Perc M, et al. Double stochastic resonance in neuronal dynamics due to astrocytes. Chaos Solitons Fractals, 2023, 168: 113140
75 Xie Y, Yao Z, Ma J. Formation of local heterogeneity under energy collection in neural networks. Sci China Tech Sci, 2023, 66: 439–455
76 Cao B, Gu H, Wang R. Complex dynamics of hair bundle of auditory nervous system (II): Forced oscillations related to two cases of steady state. Cogn Neurodyn, 2022, 16: 1163–1188
77 Nobukawa S, Wagatsuma N, Ikeda T, et al. Effect of steady-state response versus excitatory/inhibitory balance on spiking synchronization in neural networks with log-normal synaptic weight distribution. Cogn Neurodyn, 2022, 16: 871–885
78 Majhi S, Perc M, Ghosh D. Dynamics on higher-order networks: A review. J R Soc Interface, 2022, 19: 20220043
79 Ma J. Biophysical neurons, energy, and synapse controllability: A review. J Zhejiang Univ Sci A, 2023, 24: 109–129
80 Yang F, Xu Y, Ma J. A memristive neuron and its adaptability to external electric field. Chaos, 2023, 33: 023110
81 Lin H, Wang C, Yu F, et al. A review of chaotic systems based on memristive hopfield neural networks. Mathematics, 2023, 11: 1369